Supplement of Biogeosciences, 18, 1185–1201, 2021
https://doi.org/10.5194/bg-18-1185-2021-supplement

Biogeosciences
Open Access

Supplement of

Denitrification in soil as a function of oxygen availability at the microscale

Lena Rohe et al.

Correspondence to: Lena Rohe (lena.rohe@ufz.de)

Detailed information on pre-incubation, determination of water holding capacity and experimental set-up (Section 2: Material and Methods, 1. Incubation)

For pre-incubation the soil was loosely placed on a tray, adjusted to 50% water holding capacity (WHC) with a spray can and stored at room temperature in the dark for two weeks.

Additional soil cores with the same dimension were packed in an identical manner as described in the Material and Method section and fully saturated by immersion in a water bath for 24h. The water-holding capacity (v/v % WHC) for each soil material was determined after free drainage. These water volumes were taken as a reference to adjust the above-mentioned saturation levels (70, 83 and 95% WHC). Note that WHC values are not identical to water saturations expressed in v/v% water-filled pore space (WFPS), since 100%WHC covers a smaller volume than the total pore volume due to 1) air entrapment during full immersion in water and 2) drainage of the biggest pores in a pressure head range of -10 to 0 cm in a 10 cm tall, freely draining sample.

The cylindrical PVC columns containing the packed soil aggregates (698.41 cm^3) were closed tightly by sealing caps at the top and bottom. The closed column was equipped with an in- and outlet to allow flushing the headspace (69.83 cm^3) through steel capillaries (total volume 1.33 cm^3). A maximal evaporation loss during incubation of one soil core is estimated to be around 1.22 g H_2O. A temperature sensor (PT100) was installed through the centre of the lid reaching the repacked aggregates with a depth of ca 3 cm down to assure constant temperature of 20°C during incubation.

Table with average data for each treatment (WFPS and aggregate size) with average values of CO_2, N_2O and (N_2O+N_2) fluxes, O_2 saturation, total porosity, visible air content (ε_{vis}), connected air content (ε_{con}), anaerobic soil volume fraction (ansvf), simulated diffusivity (D_{sim}) and product ratio (pr) for soil from Gießen (GI) and Rotthalmünster (RM)

Table S1: Average values for CO_2, N_2O and (N_2O+N_2) fluxes, O_2 saturation, visible air content (ε_{vis}), connected air content (ε_{con}), anaerobic soil volume fraction (*ansvf*), simulated diffusivity (D_{sim}) and product ratio (*pr*) [N_2O/(N_2O+N_2)] for the two soils (Gießen (GI) and Rotthalmünster (RM)), three water saturations (water filled pore space (WFPS)) and two aggregate sizes. Standard error (n=3) is shown in the brackets.

soil	WFPS [%]	Aggregate size [mm]	CO_2-C [µg h^{-1} kg^{-1}]	N_2O-N [µg h^{-1} kg^{-1}]	(N_2O+N_2)-N [µg h^{-1} kg^{-1}]	O_2 [%air saturation]	Total porosity [-]	ε_{vis} [-]	ε_{con} [-]	*ansvf* [-]	D_{sim} [m^2 s^{-1}]	*pr* [-]
GI	63	2-4	535.71 (72.95)	0.26 (0.07)	2.94 (1.75)	47.99 (1.30)	0.21 (0.03)	0.21 (0.03)	0.20 (0.03)	<0.01 (<0.01)	1.09 10^{-06} (1.82 10^{-08})	0.34 (0.16)
GI	63	4-8	503.19 (65.9)	1.28 (0.67)	2.93 (0.45)	55.69 (1.87)	0.20 (0.02)	0.20 (0.02)	0.20 (0.02)	<0.01 (<0.01)	1.08 10^{-06} (1.56 10^{-08})	0.44 (0.09)
GI	75	2-4	617.30 (53.06)	18.01 (3.00)	35.53 (2.15)	56.48 (2.50)	0.18 (0.03)	0.13 (0.03)	0.12 (0.03)	0.04 (0.02)	1.59 10^{-08} (7.26 10^{-09})	0.52 (0.08)
GI	75	4-8	548.66 (57.25)	17.89 (1.94)	26.90 (4.42)	61.78 (2.22)	0.19 (0.03)	0.14 (0.03)	0.11 (0.04)	0.21 (0.07)	2.76 10^{-09} (2.32 10^{-09})	0.68 (0.06)
GI	85	2-4	175.33 (71.30)	18.74 (7.51)	27.20 (6.41)	33.77 (1.47)	0.18 (0.03)	0.12 (0.02)	0.03 (0.03)	0.79 (0.14)	5.59 10^{-10} (3.36 10^{-10})	0.64 (0.09)
GI	85	4-8	125.62 (21.69)	13.30 (4.45)	21.38 (1.97)	39.89 (2.55)	0.20 (0.03)	0.10 (0.02)	0.01 (0.02)	0.80 (0.09)	2.00 10^{-10} (4.00 10^{-11})	0.60 (0.10)
RM	65	2-4	144.85 (20.45)	0.02 (0.01)	NA	55.11 (2.20)	0.16 (0.03)	0.16 (0.03)	0.15 (0.03)	<0.01 (<0.01)	2.24 10^{-07} (1.39 10^{-08})	n.d.
RM	65	4-8	158.06 (21.05)	0.05 (0.03)	0.66 (0.54)	48.95 (2.56)	0.15 (0.03)	0.15 (0.03)	0.15 (0.03)	<0.01 (<0.01)	2.08 10^{-07} (2.69 10^{-08})	0.08 (0.04)
RM	78	2-4	174.29 (4.14)	4.28 (2.04)	6.86 (3.28)	59.16 (2.88)	0.14 (0.03)	0.10 (0.03)	0.09 (0.03)	0.08 (0.06)	1.03 10^{-08} (3.65 10^{-09})	0.65 (0.08)
RM	78	4-8	142.69 (26.87)	6.00 (1.18)	9.88 (1.91)	53.41 (2.60)	0.14 (0.03)	0.10 (0.03)	0.07 (0.04)	0.34 (0.22)	1.47 10^{-08} (7.34 10^{-09})	0.61 (0.05)
RM	88	2-4	50.60 (7.49)	5.07 (0.96)	8.46 (2.48)	22.61 (1.95)	0.10 (0.02)	0.06 (0.02)	0.03 (0.02)	0.69 (0.10)	3.27 10^{-11} (2.02 10^{-11})	0.64 (0.06)
RM	88	4-8	46.89 (10.41)	5.60 (1.15)	8.50 (1.92)	42.01 (2.59)	0.13 (0.03)	0.07 (0.02)	0.02 (0.01)	0.74 (0.07)	2.03 10^{-09} (1.76 10^{-09})	0.67 (0.04)

n.d.: not detectable; NA: not applicable

N_2O and CO_2 fluxes and O_2 saturation as a function of incubation time

N_2O and CO_2 fluxes (Figure S1) and O_2 saturation at 7 locations within the soil core (Figure S2) were measured during the incubation time of approximately 192h. In the beginning of incubation establishment of equilibrium was assumed and therefore 24h of measurements in the beginning of the incubation time were excluded.

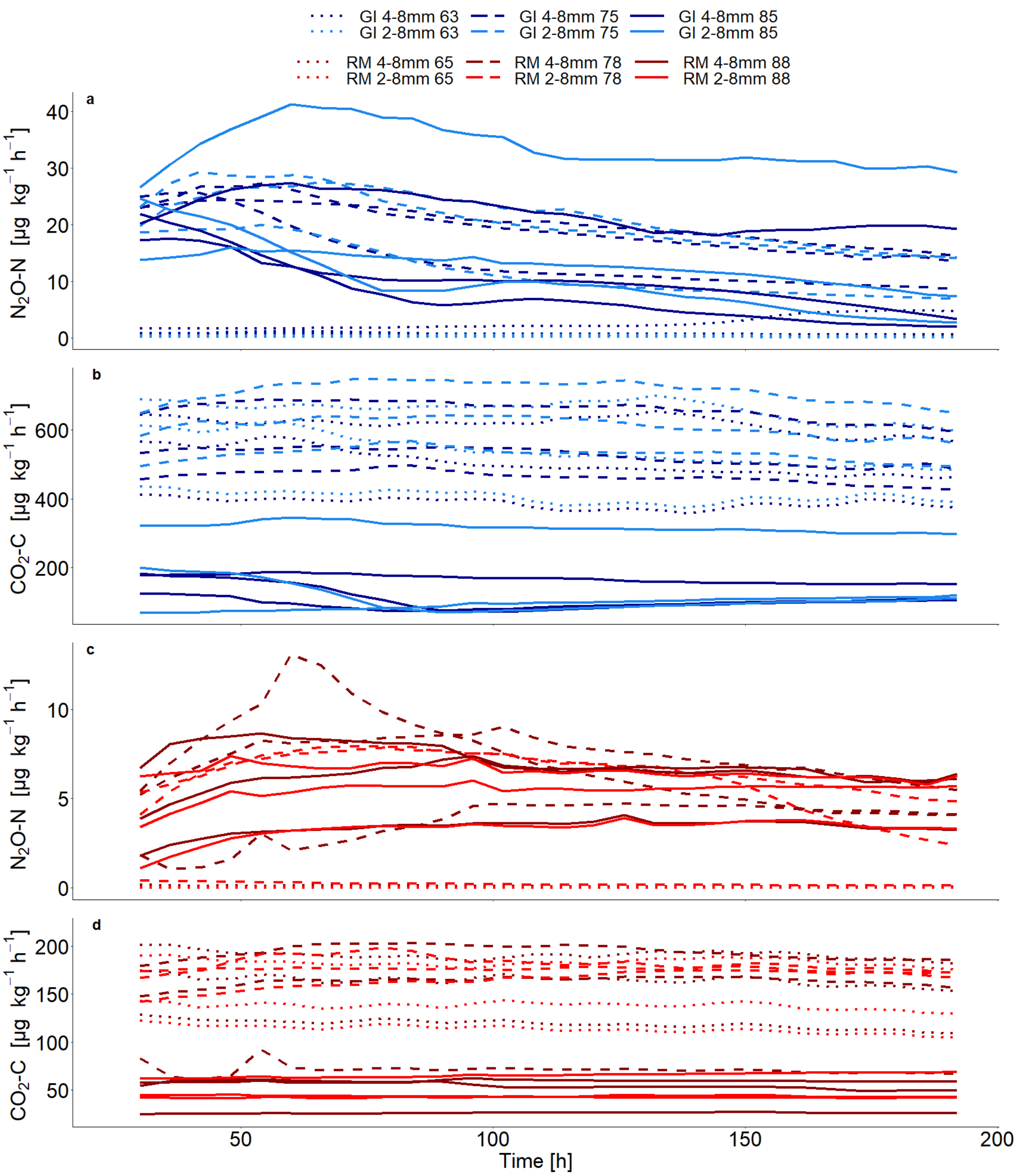

Figure S1: Average N_2O and CO_2 fluxes as a function of incubation time for soil from Rotthalmünster (RM) in red and Gießen (GI) in blue, two aggregate sizes (2-4 and 4-8 mm) and three water saturations (dotted, dashed or solid line depicted lowest (63 or 65 % water filled pore space (WFPS) with GI and RM soil, respectively), medium (75 or 78 % WFPS with GI and RM soil, respectively) and highest (85 or 88 % WFPS with GI and RM soil, respectively) water saturation, respectively) with three replicates.

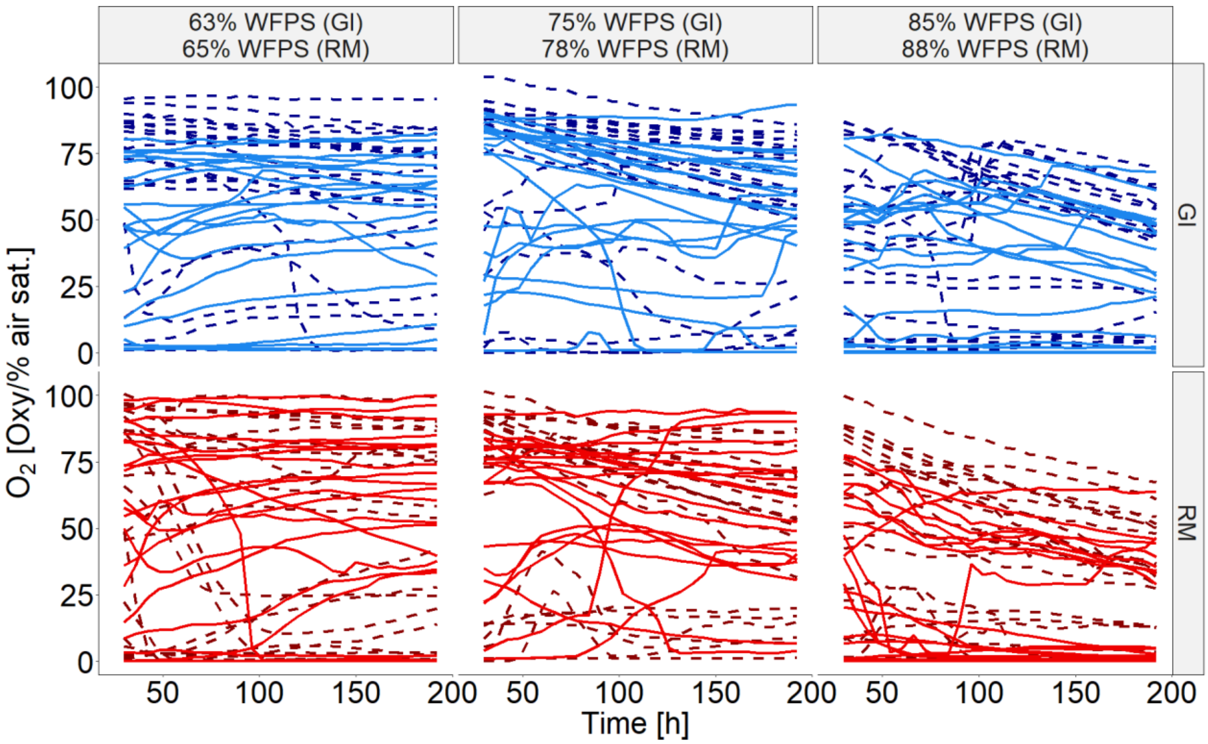

Figure S2: Average O_2 saturations measured by seven sensors per soil core as a function of incubation time for soil from Rotthalmünster (RM) in red and Gießen (GI) in blue, two aggregate sizes (2-4 and 4-8 mm (solid and dashed lines, respectively)) and three water filled pore spaces (WFPS) with three replicates each. Only the final 24h were considered for regression analysis N-gas release and X-ray CT results.

Detailed description of calculating different pools for ^{15}N

The fraction of N in N_2O ($f_p\_N_2O$) or N_2 ($f_p\_N_2$) originating from ^{15}N-labelled NO_3^- pool within one sample was calculated according to (Spott et al., 2006; Lewicka-Szczebak et al., 2013; Well et al., 2019) using the ^{15}N abundance of N_2 or N_2O measured in the analyzed gas sample (a_m), in the non-labelled N_2 in technical gas (a_{bgd}), and the calculated ^{15}N abundance of the active NO_3^- pool (a_p).

$$f_p\_N_2O = \frac{a_m - a_{bgd}}{a_p - a_{bgd}} \tag{S1}$$

$$f_p\_N_2 = \frac{a_m - a_{bgd}}{a_p - a_{bgd}} \tag{S2}$$

with

$$a_m = \frac{^{29}R + 2\,^{30}R}{2(1 + ^{29}R + ^{30}R)} \tag{S3}$$

and using the fraction of $^{30}N_2$ in the gas sample ($^{30}\chi_m$):

$$a_p = \frac{^{30}\chi_m - a_m \cdot a_{bgd}}{a_m - a_{bgd}} \tag{S4}$$

This is based on the a non-random distribution of isotopes in N_2O and N_2 (Spott et al., 2006):

$$^{30}\chi_m = \frac{^{30}R}{1+{}^{29}R+{}^{30}R} \tag{S5}$$

Thus, with $f_p\_N_2O$ the N_2O flux from denitrification (N_2O_deni) was calculated

$$N_2O\_deni = N_2O\_total * f_p\_N_2O \tag{S6}$$

The $f_p\_N_2O$ was constantly near 1 for both soils, aggregate sizes, water saturations and time points of sampling resulting in very similar N_2O_total and N_2O_deni values (Figure S3). The time resolution for N_2O_total was much higher than for isotopic analysis and therefore N_2O_total was used to calculate N_2O fluxes from denitrification and for statistical analysis.

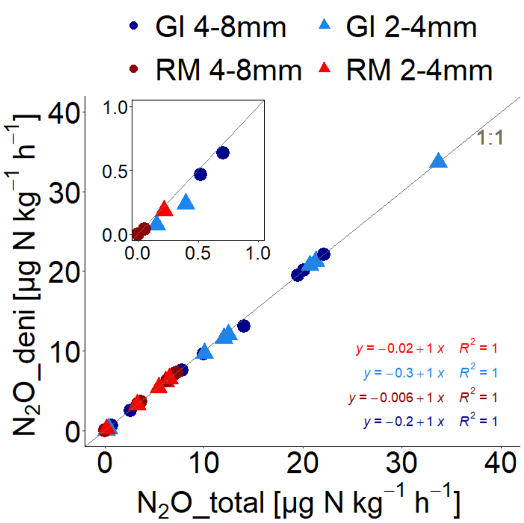

Figure S3: Comparison of total N_2O emissions (N_2O_total) captured by gas chromatography and N_2O emissions from denitrification (N_2O_deni) calculated by Eq. 6 from experimental treatments with soil from Rotthalmünster (RM) and Gießen (GI), two aggregate sizes (2-4 and 4-8 mm) and three water saturations. Goodness of fit to the 1:1 line (gray line) is expressed as slope and R^2 from linear regression. The excellent agreement implies that N_2O is produced by denitrification.

Impact of packing procedure on visible air content (ε_{vis}) and anaerobic soil volume fraction (ansvf)

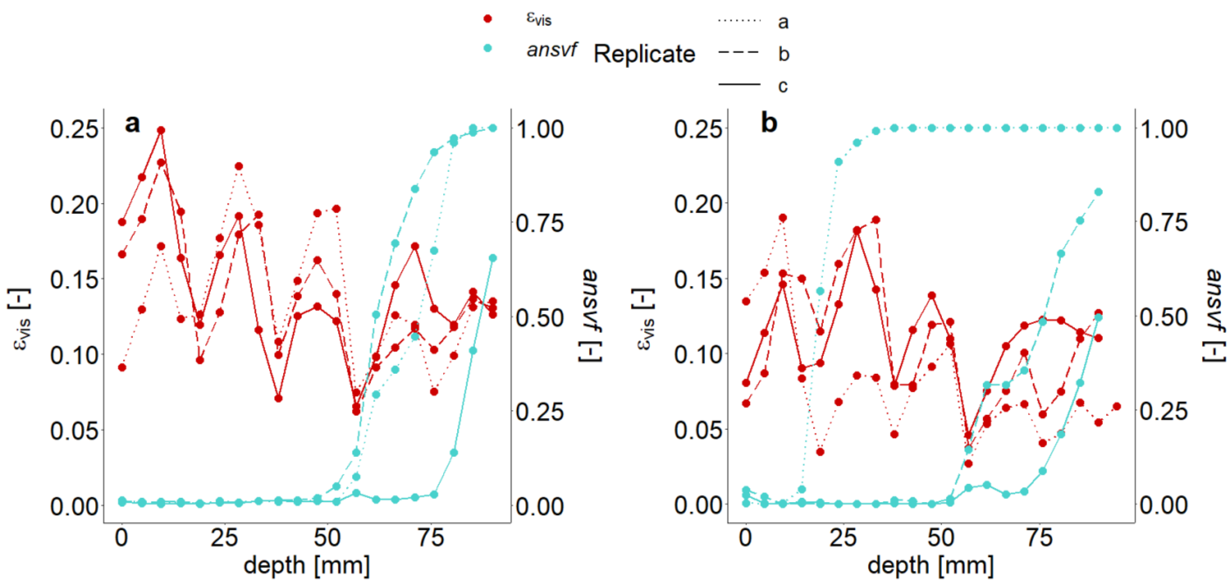

Figure S4: Visible air content (ε_{vis}) and the anaerobic soil volume fraction (*ansvf*) as a function of soil core depth for soil from (a) Gießen (GI) and (b) Rotthalmünster (RM). Shown here are examples of three replicates of repacked soil cores with aggregates of 4-8 mm size incubated at medium water saturation of 75% with GI and 78% with RM soil. Values shown here for ε_{vis} air content and *ansvf* are aggregated for 4.7 mm segments in depth. The results show that the *ansvf* increases substantially in thin soil layers with low ε_{vis} created by packing in which air continuity is lost.

Two representative examples of one treatment were chosen to illustrate the impact of packing the soil on visible air content (ε_{vis}) and anaerobic soil volume fraction (*ansvf*) (large aggregates of GI soil incubated at 75% WFPS and large aggregates of RM soil incubated at 78 % WFPS) (Figure S4). During the packing procedure, intervals of 2 cm were the best option to adjust the target material-specific bulk densities and water saturations within the soil core. The average ε_{vis} did not differ between replicates of one treatment (Figure 4), but decreased with increasing depth of the packed soil core and was extremely reduced at the top of one packing interval (Figure S4). This varying compaction in different layers affected also the *ansvf* of each repacked core (Figure S4). The *ansvf* dramatically increased in layers, where lowest ε_{vis} was observed. In some cases, the *ansvf* even reached 1, i.e. complete exclusion from connected air-filled pores.

Detailed information on simulated diffusivity (D_{sim})

Diffusivity was simulated for individual aggregates as well as for the entire soil core (bulk diffusivity) directly on segmented X-ray CT data on a workstation with Intel® Xeon® CPUs (E7-8867v4, 2.46Hz, 36 cores) and 6.1TB RAM by solving the Laplace equation with the DiffuDict module in the GeoDict 2019 Software (Math2Market GmbH, Kaiserslautern, Germany). A hierarchical approach was used to estimate the effective diffusivity of the wet soil matrix by simulating Laplace diffusion on cubes contained in individual soil aggregates with the Explicit Jump solver assuming free diffusion in the visible pore space, a completely impermeable background and symmetric boundary condition on all sides (Wiegmann and Zemitis, 2006; Wiegmann and Bube, 2000). The resulting effective diffusion coefficient is expressed as a percentage of the diffusion coefficient in the free fluid and was in the range of $6.6\ 10^{-4} \pm 3.7\ 10^{-4}$% and $2.4\ 10^{-2} \pm 1.3\ 10^{-2}$% for wet aggregates of RM and GI soil, respectively. For the soil cores with <70% WFPS the visible pore space in the high-resolution aggregate images is assumed to be air-filled, whereas for soil cores with ≥75% WFPS it is assumed to be water-filled, which is justified by the fact that 1) the air-filled porosity at <70% WFPS in individual aggregates (RM: 17.6%, GI: 23.1%) exceeds the visible pore space in low-resolution soil core images (RM: 15.8%, GI: 20.6%) and 2) that in contrast to the higher moisture levels no free water could be identified at the column scale with air-filled porosity at <70% WFPS. Thus, the effective diffusion coefficient for soil matrix is determined with respect to the oxygen diffusion coefficient (D_{O2}) at 2% O_2 in pure air ($2.03\ 10^{-5}$ m² s^{-1}) and in pure water ($1.97\ 10^{-9}$ m² s^{-1}) at 20°C, respectively (http://compost.css.cornell.edu/oxygen/oxygen.diff.air.html).

Another series of diffusion experiments was modeled with the Explicit Jump solver on the entire soil cores (1550x1550x [1500-1600] voxels) with the effective diffusion coefficient of the soil matrix taken from aggregate simulations, an impermeable exterior, impermeable mineral grains (GI only) and the diffusion coefficient of oxygen in air and water (≥70% WFPS only) in the respective material classes. In order to save memory, periodic boundary conditions were assumed on all sides. This is irrelevant for lateral boundaries as they are blocked by the impermeable exterior anyway, but may lead to a lower effective diffusion coefficient, since the spatial distribution of materials at the top and bottom of the domain do not match, which imposes an additional diffusion barrier. The reduction by this discontinuity was in the range of $5.1\ 10^{-9}$ to $6.7\ 10^{-8}$ $m^2\ s^{-1}$ in small test images (500^3 voxels) from all soil materials and saturations.

Product ratio (pr) as a function of time

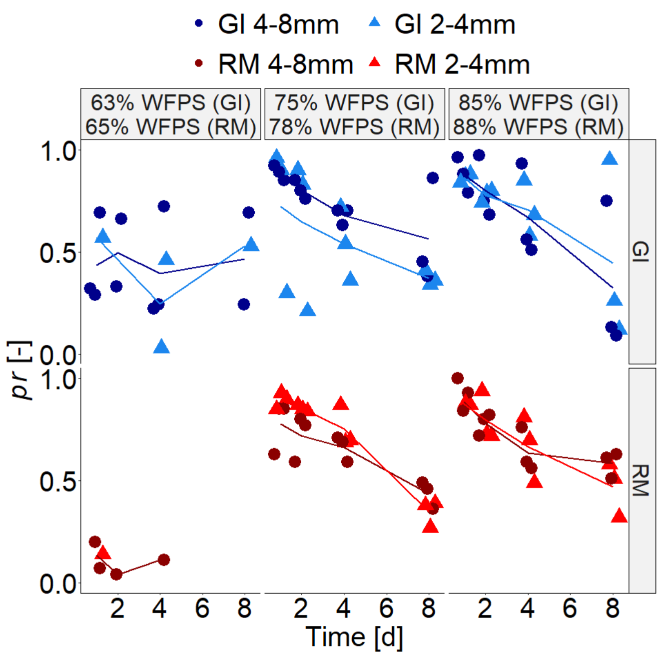

Figure S5: Product ratio (*pr*) [$N_2O/(N_2O+N_2)$] as a function of time for soil from Gießen (GI) in blue and Rotthalmünster (RM) in red with aggregates of 2-4 mm and 4-8mm size incubated at three water filled pore spaces (WFPS). The lines connect the average values of three replicates (large and small aggregates, respectively). The *pr* decreases gradually over time due to a relative increase in N_2.

Correlation between ansvf and gas emissions and concentrations

The correlation of *ansvf* with average gas fluxes and internal O_2 concentrations is shown in Figure S6. Since the drop in CO_2 release at the highest water saturations coincided with an escalating *ansvf*, the relation between the two was highly correlated (Spearman's R>-0.7 and p=0.04) for all soils and aggregate sizes (Figure S6a), but with different slopes for both soils due to vastly different SOM contents. The correlation of *ansvf* with N_2O is weaker (Spearman's 0.6<R<0.77) and on the verge of being significant (p≤0.1) (Figure S6c). However, the correlation of *ansvf* with (N_2O+N_2) release is even worse (p>0.2), so the mechanisms that govern N_2O and (N_2O+N_2) release must be more complex (Figure S6c, d). As expected the average O_2 saturation decreases with increasing *ansvf* (Figure S6b). Yet, correlation is lower than for CO_2 (Spearman's -0.6<R<-0.2, but p>0.2), likely due to limited representativeness of average O_2 concentrations derived from a few point measurements.

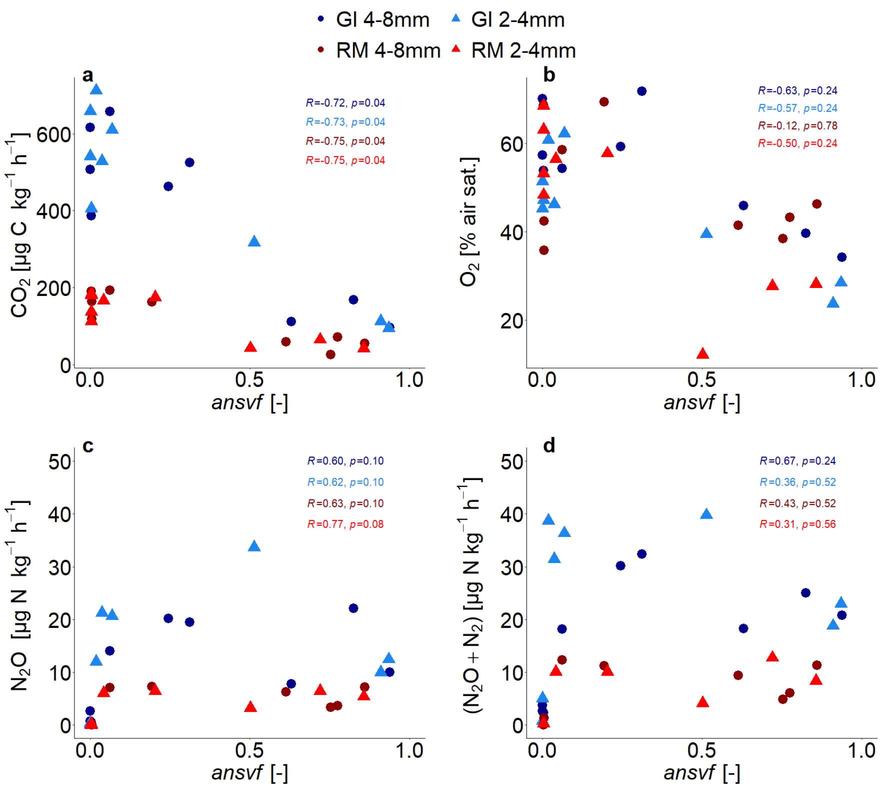

Figure S6: Average (a) CO_2, fluxes (b) O_2 saturation, (c) N_2O and (d) (N_2O+N_2) fluxes as a function of anaerobic soil volume fraction (*ansvf*) for soil from Rotthalmünster (RM) and Gießen (GI) and two aggregate sizes (2-4 and 4-8 mm) for three individual replicates. The Spearman's rank correlation coefficient (*R)* indicate the extent of monotonic relation between the ranks of both variables. The associated p-values (*p*) were corrected for multiple comparison according to Benjamini and Hochberg (1995).

Correlation matrix between all variables

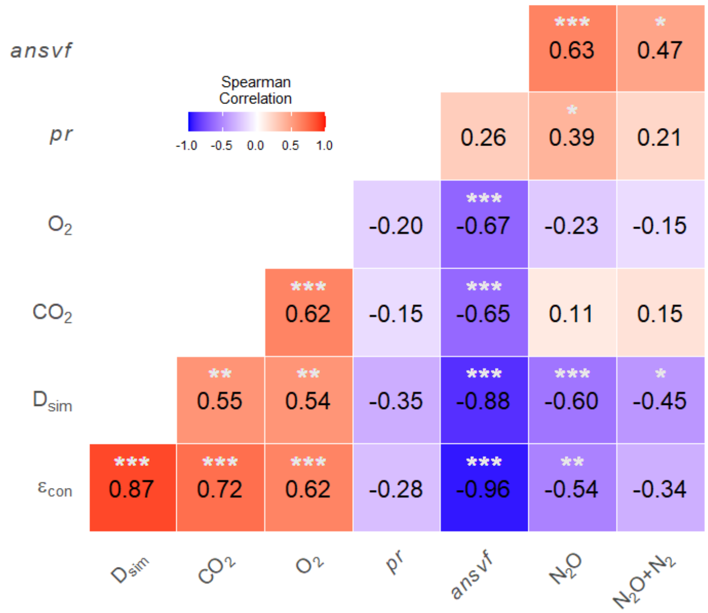

Figure S7: Correlation matrix of Spearman's rank correlation showing coefficients (*R*) between two measured variables (N_2O, (N_2O+N_2) or CO_2 fluxes, anaerobic soil volume fraction (*ansvf*), product ratio (*pr*), O_2 saturation (O_2), simulated diffusivity (D_{sim}) or connected air content (ε_{con})) in one cell with pairwise deletion of missing values. Asterisks indicate the statistical significance with significance levels of *p ≤ 0.05, **p ≤ 0.005, ***p ≤ 0.001 for adjusted p-values according to the method of Benjamini and Hochberg (1995). Color scheme indicate low (light colors) or strong (intensive colors) correlation as well as positive (red) or negative (blue) correlation.

Explanatory variables for denitrification

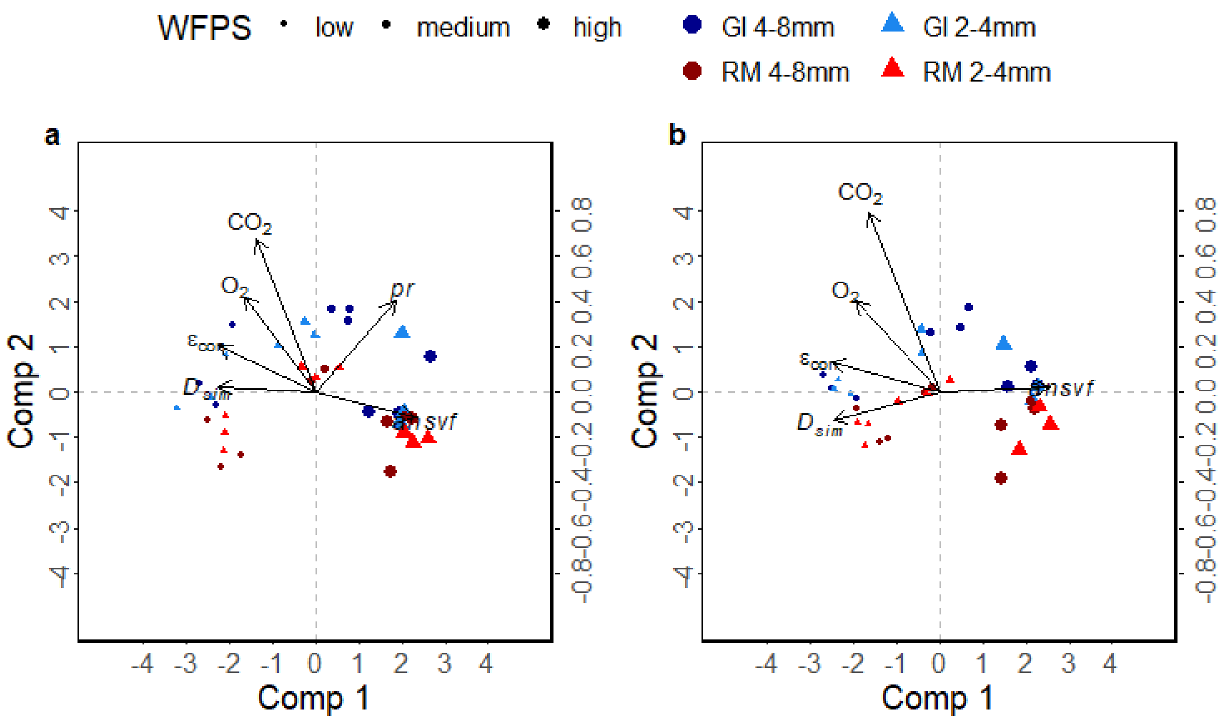

Figure S8: Biplot of the PLSR results for response variables N_2O (a) and (N_2O+N_2) fluxes (b) showing x-scores and x-loadings of two components (Comp 1 and Comp 2). The x- and y- axis represent values of the scores for soil from Gießen (GI) in blue and Rotthalmünster (RM) in red with aggregates of 2-4 mm (triangles) and 4-8 mm size (circles) incubated at three water saturations depicted by the size of symbols. The second y-axis represents values for the loadings (predictors and arrows) to show the influence of variables on the components.

The regression equations with R^2 values and a confidence interval of 95% in square brackets resulting from PLSR with CO_2, (*pr*) and *ansvf* as explanatory variables to predict N_2O or (N_2O+N_2) fluxes of the present study for data after log- or logit transformation:

$$\log(N_2O) = 0.63\log(CO_2) + 0.41\ \mathrm{logit}(ansvf) + 0.64\,pr - 0.38\log(D_{sim}) - 0.22\,\varepsilon_{con} + 0.12\,O_2;$$

$$R^2 = 0.82\ [0.65\text{-}0.91] \qquad \text{(S7)}$$

$$\log(N_2O + N_2) = 1.1\log(CO_2) + 0.70\ \mathrm{logit}(ansvf) - 0.65\log(D_{sim}) - 0.37\,\varepsilon_{con} + 0.10\,O_2\ ;$$

$$R^2 = 0.78\ [0.62\text{-}0.85] \qquad \text{(S8)}$$

Empirical models to calculate the diffusivity of the soil cores

It is assumed, that the total porosity (Φ) was unaffected by the packing procedure, whereas the air content (ε) is expected to differ from the theoretic value due to compact regions and intervals caused by the packing (Figure S4). Following from this, the target bulk density of the repacked soil cores was used to calculate Φ (0.62 or 0.51 for GI and RM soil, respectively), while CT-derived ε was used. This enabled to calculate diffusivity based on the frequently used model of Millington and Quirk (1960), Millington and Quirk (1961), Moldrup et al. (2000) and also according to the model of Deepagoda et al. (2011)

(Table S2, Figure S9). As expected, diffusivity from these models has a lower explanatory power for N_2O and (N_2O+N_2) release compared to D_{sim} of the present study (3D simulation) (Table S2). Higher diffusivities for treatments ≥75% WFPS from empirical models (D_{emp}) compared to D_{sim} result from heterogeneities in compaction of the repacked soil core as described earlier (Figure S4, Figure S9), while empirical models were developed for natural soils that very likely possess higher air continuity at low air content. These empirical models only take averages for porosity and water-filled pores into account (Millington and Quirk, 1961; Moldrup et al., 2000) (Figure S9, Table S2), whereas heterogeneities in compaction are explicitly considered in 3D diffusivity simulations (D_{sim}).

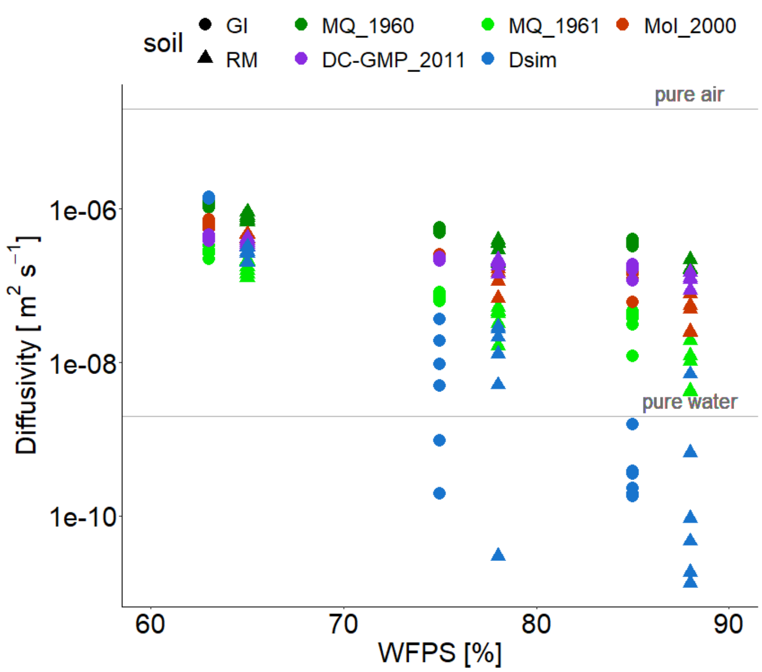

Figure S9: Simulated diffusivities (D_{sim}) of the present study (blue circle) and calculated diffusivities as a function of WFPS for both soils (Rotthalmünster (RM) and Gießen (GI)). Models used to calculate diffusivity are published by Millington and Quirk (1960) (MQ_1960, green circle), Millington and Quirk (1961) (MQ_1961, light green circle), Moldrup et al. (2000) (Mol_2000, red circle) and Deepagoda et al. (2011) (DC_GMP_2011, purple circle). According to the calculations of the present study diffusivity in free air (D_0) was assumed to be 2.03 10^{-5} m^2 s^{-1}.

Table S2: Explained variability (expressed as R^2) for response variables N_2O and (N_2O+N_2) with confidence interval of 95% in square brackets for N_2O and (N_2O+N_2) release obtained from partial least square regression (PLSR) using explanatory variables CO_2, diffusivity (and product ratio (*pr*) for N_2O as response variable only). This was done to assess possibilities to substitute one of the most important explanatory variables (*ansvf*) by diffusivity. Data were pooled for both soils (RM and GI), WFPS treatments and aggregate sizes (n= 36). Diffusivity was obtained by 3D simulation of the present study (D_{sim}) or existing soil gas diffusivity models were used to calculate diffusivity, using total porosity (Φ) and air content (ε) while diffusivity in free air (D_0) is assumed to be 2.03 10^{-5} m^2 s^{-1}.

method	Equation to calculate diffusivity D_{emp} [m^2 s^{-1}]	R^2 with response variable N_2O	R^2 with response variable (N_2O+N_2)
Present study[1]	D_{sim}	0.59 [0.34-0.78]	0.63 [0.39-0.78]
Millington & Quirk (1961) [1]	$(\varepsilon^{10/3}/\Phi^2)\ D_0$	0.46 [0.20-0.69]	0.57 [0.28-0.78]
Millington & Quirk (1960) [1]	$(\varepsilon^2/\Phi^{2/3})\ D_0$	0.48 [0.22-0.70]	0.52 [0.21-0.74]
Moldrup et al. (2000)[1]	$\varepsilon^{1.5}\ (\varepsilon/\Phi)\ D_0$	0.59 [0.29-0.79]	0.54 [0.24-0.75]
Deepagoda et al. (2011)[1]	$0.1[2(\varepsilon/\Phi)^3+0.04(\varepsilon/\Phi)]\ D_0$	0.52 [0.27-0.73]	0.69 [0.42-0.82]
theoretic air content[2]	ε_t	0.55 [0.30-0.76]	0.78 [0.57-0.90]
no diffusivity[3]	-	0.48 [0.16-0.71]	0.07

[1]PLSR with CO_2 and diffusivity (and product ratio (*pr*)) as explanatory variables and N_2O or (N_2O+N_2) as response variables.

[2]Diffusivity substituted by the theoretic air content (ε_t) targeted during packing in PLSR resulting in CO_2 and ε_t (and product ratio (*pr*)) as explanatory variable for N_2O and for (N_2O+N_2).

[3]Diffusivity was excluded in PLSR resulting in CO_2 (and product ratio (*pr*)) as explanatory variable for N_2O and for (N_2O+N_2). Because CO_2 was the single explanatory variable for (N_2O+N_2) a simple linear model was used to estimate R^2.

Calculation of anaerobic soil volume fraction (ansvf) by (N_2O+N_2) fluxes from oxic and anoxic incubations

To calculate an anaerobic soil volume fraction within the soil cores (*ansvf*$_{cal}$) independently from the X-ray CT imaging derived *ansvf*, parallel oxic and anoxic incubations were conducted using a different suite of larger repacked soil cores. The conditions for incubations were very similar in soil cores as described before (in the Methods section and Supplementary Material) for oxic incubation. Deviations from the experimental protocol were the dimension of the soil core (10x14.4 cm), unspecific sieving (>10 mm), a flow rate of 20 mL/min and a target saturation of 75% WFPS for both soils (GI and RM). Soil material for all incubations was obtained from the same batches. Batches consisted of approx. 2000kg sieved, homogenized and air-dried soil stored at 6°C that had been collected and prepared to allow the study of comparable soil samples in various labs during several years. After three weeks with oxic incubation using a technical gas (20% O_2 and 2% N_2 in pure He) the atmospheric conditions were switched to anoxic conditions (2% N_2 in pure He). N_2O and N_2 fluxes were quantified using the ^{15}N labelling approach as described before. A comparison of oxic and anoxic (N_2O+N_2) fluxes under these comparable conditions is possible because *ansvf*$_{cal}$ assumes that actual denitrification is linearly related to *ansvf* and that the specific anoxic denitrification rate is homogenous, i.e. would be identical at any location within the soil.

The calculated *ansvf* ($ansvf_{cal}$) derived from incubation (N_2O+N_2) fluxes with oxic ($(N_2O+N_2)_{oxic}$) and anoxic ($(N_2O+N_2)_{anoxic}$) conditions is thus (Table S3):

$$ansvf_{cal} = \frac{(N_2O+N_2)_{oxic}}{(N_2O+N_2)_{anoxic}} \quad (9)$$

Table S3: Average (N_2O+N_2) fluxes with oxic conditions ($(N_2O+N_2)_{oxic}$) and with anoxic conditions ($(N_2O+N_2)_{anoxic}$) (n=4) from parallel incubations for soils from Rotthalmünster (RM) and Gießen (GI). Anoxic conditions were established after 3 weeks of oxic incubation. Average (N_2O+N_2) fluxes from oxic and anoxic incubations served to calculate the anaerobic soil volume fraction ($ansvf_{cal}$) (Eq. 9). In comparison to the $ansvf_{cal}$, *ansvf* derived from X-Ray CT imaging from the present study is also presented.

soil	WFPS	Aggregate size [mm]	$(N_2O+N_2)_{oxic}$ [µg N h^{-1} kg^{-1}] (parallel incubation)	$(N_2O+N_2)_{anoxic}$ [µg N h^{-1} kg^{-1}] (parallel incubation)	$ansvf_{cal}$	*ansvf* (present study)
RM	75-78	2-8	14±10	60±2	0.24±0.16	0.21
GI	75	2-8	61±97	136±18	0.45±0.71	0.13

Table with data for each replicate with average values of CO_2, N_2O and (N_2O+N_2) fluxes, O_2 saturation, total porosity, visible air content, connected air content (ε_{con}), anaerobic soil volume fraction (ansvf), diffusivity (D_{sim}) and product ratio (pr)

Table S4: Average values of CO_2, N_2O and (N_2O+N_2) fluxes, O_2 saturation, total porosity, visible air content (*ε_{vis}*), connected air content (ε_{con}), anaerobic soil volume fraction (*ansvf*), diffusivity (*D_{sim}*) and product ratio (*pr*, [$N_2O/(N_2O+N_2)$]) for the two soils (Gießen (GI) and Rotthalmünster (RM)), three water saturations and two aggregate sizes for three replicates. Standard error of the mean is shown in the brackets.

soil	WFPS[%]	Aggre-gate size [mm]	Rep li-cate	CO_2-C [µg h^{-1} kg^{-1}] (n=28)	N_2O-N [µg h^{-1} kg^{-1}] (n=28)	(N_2O+N_2) [µg N h^{-1} kg^{-1}] (n=3)	O_2 [%air saturation] (n=7)	Total poro-sity [-]	ε_{vis} [-]	ε_{con} [-]	*ansvf* [-]	D_{sim} [m^2 s^{-2}]	*pr* (n= 1-3)
GI	63	2-4	a	406.30 (3.24)	0.22 (<0.01)	NA	47.19 (12.13)	0.20	0.20	0.19	0.003	$1.10\ 10^{-06}$	n.d.
GI	63	4-8	a	387.38 (2.83)	0.52 (0.07)	2.36 (NA)	53.79 (13.07)	0.19	0.19	0.19	0.004	$1.05\ 10^{-06}$	0.22 (n.d)
GI	75	2-4	a	528.74 (3.73)	21.28 (0.84)	31.45 (7.65)	46.27 (11.64)	0.18	0.13	0.12	0.037	$2.89\ 10^{-08}$	0.68 (0.14)
GI	75	4-8	a	463.32 (3.42)	20.14 (0.60)	30.21 (5.65)	59.24 (11.59)	0.19	0.14	0.10	0.246	$7.50\ 10^{-10}$	0.67 (0.12)
GI	85	2-4	a	317.57 (2.55)	33.68 (0.76)	39.78(3.94)	39.43 (9.42)	0.17	0.11	0.07	0.513	$1.54\ 10^{-10}$	0.85 (0.06)
GI	85	4-8	a	168.18 (2.30)	22.11 (0.59)	25.03 (2.79)	39.66 (12.20)	0.18	0.08	0.02	0.824	$1.40\ 10^{-10}$	0.88 (0.07)
GI	63	2-4	b	542.08 (8.62)	0.15 (<0.01)	5.09 (NA)	45.32 (10.48)	0.22	0.22	0.21	0.001	$1.11\ 10^{-06}$	0.03 (n.d.)
GI	63	4-8	b	506.33 (7.33)	0.71 (0.01)	2.62 (0.33)	57.38 (11.56)	0.21	0.21	0.21	0.001	$1.11\ 10^{-06}$	0.27 (0.03)
GI	75	2-4	b	610.95 (4.95)	20.73 (0.98)	36.37 (10.48)	62.33 (6.19)	0.18	0.13	0.12	0.068	$1.49\ 10^{-08}$	0.57 (0.14)
GI	75	4-8	b	525.22 (4.49)	19.51 (0.83)	32.34 (7.77)	71.78 (7.66)	0.19	0.14	0.10	0.312	$1.52\ 10^{-10}$	0.60 (0.12)
GI	85	2-4	b	95.47 (3.03)	12.48 (0.46)	22.98 (7.01)	28.45 (10.02)	0.18	0.12	<0.01	0.935	$1.23\ 10^{-09}$	0.54 (0.15)
GI	85	4-8	b	97.08 (2.71)	9.99(0.72)	20.82 (9.16)	34.16 (9.45)	0.18	0.11	<0.01	0.938	$1.82\ 10^{-10}$	0.48 (0.18)
GI	63	2-4	c	658.77 (5.38)	0.40 (0.01)	0.80 (0.10)	51.43 (9.55)	0.21	0.21	0.20	<0.001	$1.05\ 10^{-06}$	0.50 (0.04)
GI	63	4-8	c	615.87 (4.61)	2.63 (0.22)	3.81 (1.00)	70.19 (6.95)	0.20	0.20	0.20	<0.001	$1.08\ 10^{-06}$	0.69 (0.02)
GI	75	2-4	c	712.21 (5.89)	12.02 (0.90)	38.77 (10.84)	60.83 (8.62)	0.19	0.13	0.13	0.018	$3.88\ 10^{-09}$	0.31 (0.05)
GI	75	4-8	c	657.43 (5.30)	14.03 (1.07)	18.15 (4.37)	54.30 (14.00)	0.19	0.14	0.13	0.063	$7.38\ 10^{-09}$	0.77 (0.05)
GI	85	2-4	c	112.95 (7.61)	10.04 (1.16)	18.83 (9.96)	23.67 (10.43)	0.18	0.12	<0.01	0.910	$2.98\ 10^{-10}$	0.53 (0.21)
GI	85	4-8	c	111.59 (6.66)	7.80 (1.10)	18.29 18.87)	45.84 (10.25)	0.23	0.12	0.02	0.629	$2.75\ 10^{-10}$	0.43 (0.18)
RM	65	2-4	a	137.89 (0.65)	0.01 (n.d.)	NA	68.61 (7.14)	0.15	0.15	0.14	0.004	$2.51\ 10^{-07}$	n.d.
RM	65	4-8	a	164.47 (0.90)	0.10 (<0.01)	NA	35.75 (12.64)	0.16	0.16	0.15	0.005	$2.47\ 10^{-07}$	n.d.
RM	78	2-4	a	180.88 (1.57)	0.22 (0.01)	0.31 (0.10)	63.18 (10.22)	0.14	0.11	0.10	0.004	$1.66\ 10^{-08}$	0.71 (0.16)
RM	78	4-8	a	71.12 (1.00)	3.65 (0.21)	6.11 (1.32)	43.27 (11.97)	0.14	0.08	0.03	0.775	$2.34\ 10^{-11}$	0.60 (0.06)
RM	88	2-4	a	43.12 (0.19)	3.27 (0.11)	4.21 (0.73)	12.13 (8.11)	0.10	0.07	0.05	0.502	$7.31\ 10^{-11}$	0.78 (0.11)
RM	88	4-8	a	26.20 (0.12)	3.36 (0.08)	4.83 (0.48)	38.36 (11.27)	0.10	0.05	0.02	0.753	$5.53\ 10^{-09}$	0.70 (0.04)
RM	65	2-4	b	113.43 (0.75)	0.04 (<0.01)	NA	48.38 (11.00)	0.17	0.17	0.16	0.003	$2.10\ 10^{-07}$	n.d.
RM	65	4-8	b	118.83 (0.85)	0.05 (<0.01)	1.31 (NA)	42.40 (11.85)	0.15	0.15	0.14	0.005	$1.57\ 10^{-07}$	0.04 (n.d.)
RM	78	2-4	b	166.66 (1.95)	6.12 (0.30)	10.14 (3.34)	56.52 (8.62)	0.13	0.10	0.08	0.042	$1.02\ 10^{-08}$	0.60 (0.17)
RM	78	4-8	b	163.13 (0.92)	7.31 (0.19)	11.25 (1.98)	69.43 (9.15)	0.14	0.11	0.09	0.193	$2.13\ 10^{-08}$	0.65 (0.10)
RM	88	2-4	b	43.09 (0.20)	5.43 (0.09)	8.39 (1.01)	28.13 (9.56)	0.09	0.07	0.01	0.856	$1.04\ 10^{-11}$	0.64 (0.07)
RM	88	4-8	b	55.12 (0.70)	7.16 (0.16)	11.30 (1.74)	46.26 (9.60)	0.14	0.07	0.01	0.860	$3.65\ 10^{-11}$	0.63 (0.09)

RM	65	2-4	c	183.25 (0.70)	n.d.	NA	53.25 (14.68)	0.17	0.17	0.16	0.003	$2.10\ 10^{-07}$	n.d.
RM	65	4-8	c	190.89 (0.82)	n.d.	NA	68.71 (15.40)	0.16	0.16	0.15	0.003	$2.19\ 10^{-07}$	0.11 (n.d.)
RM	78	2-4	c	175.34 (0.30)	6.51 (0.18)	10.12 (2.29)	57.79 (6.92)	0.14	0.11	0.08	0.203	$4.00\ 10^{-09}$	0.64 (0.13)
RM	78	4-8	c	193.83 (1.27)	7.04 (0.46)	12.29 (3.66)	58.57 (12.57)	0.14	0.11	0.10	0.062	$2.28\ 10^{-08}$	0.57 (0.12)
RM	88	2-4	c	65.58 (0.40)	6.53 (0.07)	12.80 (2.94)	27.69 (8.80)	0.11	0.05	0.02	0.720	$1.45\ 10^{-11}$	0.51 (0.12)
RM	88	4-8	c	549.33 (0.22)	6.27 (0.12)	9.36 (1.24)	41.41 (9.23)	0.16	0.08	0.03	0.613	$5.19\ 10^{-10}$	0.67 (0.08)

n.d.: not detectable; NO and N_2 concentration was below detection limit for IRMS analysis, thus calculation of *pr* was impossible. NA: not applicable

References

Benjamini, Y., and Hochberg, Y.: Controlling the false discovery rate: a practical and powerful approach to multiple testing, Journal of the Royal Statistical Society. Series B (Methodological), 57, 289-300, 1995.

Deepagoda, T., Moldrup, P., Schjonning, P., de Jonge, L. W., Kawamoto, K., and Komatsu, T.: Density-corrected models for gas diffusivity and air permeability in unsaturated soil, Vadose Zone J., 10, 226-238, https://doi.org/10.2136/vzj2009.0137, 2011.

Lewicka-Szczebak, D., Well, R., Giesemann, A., Rohe, L., and Wolf, U.: An enhanced technique for automated determination of ^{15}N signatures of N_2, (N_2+N_2O) and N_2O in gas samples, Rapid Commun. Mass Spec., 27, 1548-1558, https://doi.org/10.1002/rcm.6605, 2013.

Millington, R., and Quirk, J. P.: Permeability of porous solids, Transactions of the Faraday Society, 57, 1200-&, https://doi.org/10.1039/tf9615701200, 1961.

Millington, R. J., and Quirk, J. M.: Transport in porous media, in: F.A. Van Beren et. al (ed.), Trans. Int. Congr. Soil Sci., 7th, Madison, WI. 14–21 Aug, Elsevier, Amsterdam, 97–106, 1960.

Moldrup, P., Olesen, T., Gamst, J., Schjonning, P., Yamaguchi, T., and Rolston, D. E.: Predicting the gas diffusion coefficient in repacked soil: Water-induced linear reduction model, Soil Sc. Soc. Am. J., 64, 1588-1594, https://doi.org/10.2136/sssaj2000.6451588x, 2000.

Spott, O., Russow, R., Apelt, B., and Stange, C. F.: A ^{15}N-aided artificial atmosphere gas flow technique for online determination of soil N_2 release using the zeolite Köstrolith SX6®, Rapid Commun. Mass Spec., 20, 3267-3274, https://doi.org/10.1002/rcm.2722, 2006.

Well, R., Burkart, S., Giesemann, A., Grosz, B., Köster, J. R., and Lewicka-Szczebak, D.: Improvement of the ^{15}N gas flux method for in situ measurement of soil denitrification and its product stoichiometry, Rapid Commun. Mass Spec., 33, 437-448, https://doi.org/10.1002/rcm.8363, 2019.

Wiegmann, A., and Bube, K. P.: The explicit-jump immersed interface method: Finite difference methods for PDEs with piecewise smooth solutions, SIAM J. Numer. Anal., 37, 827-862, https://doi.org/10.1137/S0036142997328664, 2000.

Wiegmann, A., and Zemitis, A.: EJ-HEAT: A fast explicit jump harmonic averaging solver for the effective heat conductivity of composite materials, Berichte des Fraunhofer ITWM, 94, 2006.